Available online at www.sciencedirect.com
ScienceDirect
Catalysis Today 133–135 (2008) 400–405
CATALYSIS TODAY
www.elsevier.com/locate/cattod

Hydrogenation of synthetic PYGAS—Effects of zirconia on Pd/Al_2O_3

Alexandre Barros Gaspar [a], Gabriel Rosa dos Santos [b], Roberta de Souza Costa [b], Mônica Antunes Pereira da Silva [b,*]

[a] *Instituto Nacional de Tecnologia, Av. Venezuela 82, Sl. 518 Centro, Rio de Janeiro, RJ 20084-310, Brazil*
[b] *Escola de Química, UFRJ, Centro de Tecnologia, Bloco E, Ilha do Fundão, Rio de Janeiro, RJ 21949-900, Brazil*

Available online 1 February 2008

Abstract

Pd-based catalysts supported on ZrO_2 and $xZrO_2/Al_2O_3$ (x = 0, 10 and 20 wt.%) were prepared and characterized by X-ray diffraction, diffuse reflectance spectroscopy, temperature programmed reduction and chemisorption of H_2. Catalysts were evaluated via hydrogenation of a model mixture representative of pyrolysis gasoline, containing styrene, 1,7-octadiene, 1-octene and dicyclopentadiene in a batch reactor operated at 30 bar and 60 °C. The Pd/Al_2O_3 catalyst presented the higher metallic dispersion and hydrogenation activity. In spite of the occurrence of reduction at high temperatures and no H_2 consumption at room temperature, the catalyst Pd/ZrO_2 presented the lowest dispersion, ascribed to the weak Pd–ZrO_2 interaction. The initial hydrogenation rate of styrene was the highest as compared to that of other components. The results suggest that hydrogenation of 1,7-octadiene to octane occurs via series reaction, with 1-octene as intermediate.

Keywords: Pyrolysis gasoline hydrogenation; Pd; ZrO_2

1. Introduction

Pyrolysis gasoline (PYGAS) is a typical sub-product of high temperature naphtha pyrolysis [1,2]. PYGAS is unstable due to the presence of unsaturated compounds, such as mono and di-olefins, in addition to styrene, that are gum agents. The classical process to stabilize PYGAS is via catalytic hydrogenation of these reactive species, developed in two steps [2]. In the first step, the selective hydrogenation of mono-olefins, di-olefins and styrene is carried out, using Pd or nickel catalysts supported on alumina (Al_2O_3) and mild temperature and pressure conditions [3]. The second step occurs over catalysts like cobalt molybdate supported on Al_2O_3 in order to remove sulfur and additional olefins hydrogenation using more severe conditions [4]. According to new environmental regulations in order to reduce the content of aromatic hydrocarbons in gasoline, recently, the hydrodearomatization of pyrolysis gasoline has received great attention [5,6].

Styrene hydrogenation in particular has been studied with Pd and Ni catalysts using mild conditions [2,7–13]. This process has been used as model reaction to represent PYGAS hydrogenation because it is one of the less reactive components to be hydrogenated [7]. According to Nijhuis et al. [7], the reaction initially proceeds via a zero order in styrene and changes to a first order when complete conversion is being approached for Pd/Al_2O_3 catalysts, as predicted by the Langmuir–Hinshelwood kinetic model.

In the last years, zirconium oxide has been largely used as support in catalysts for many reactions, such as hydrocarbons hydrogenation, methanation and methane reforming [14–16]. The specific behavior of zirconia (ZrO_2) in these reactions is ascribed to its high thermal stability, presence of acid and basic surface sites and oxygen storage capacity. However, ZrO_2 has low surface area, typically about 50 m^2/g, comparing unfavorably with other conventional supports, such as Al_2O_3 and SiO_2 (100–600 m^2/g), and is more expensive. Thus, the dispersion of ZrO_2 over such oxides is an attractive option, allowing obtaining the properties of ZrO_2 with high surface area and mechanical stability of Al_2O_3 or silica [17].

Preparation and characterization of ZrO_2/Al_2O_3 systems have been studied [18–20]. Damyanova et al. [18] reported that the monolayer of ZrO_2 over Al_2O_3 is formed in the range 13–17 wt.% ZrO_2, resulting supports with the following textural

* Corresponding author. Fax: +55 21 25627567.
E-mail address: monica@eq.ufrj.br (M.A.P. da Silva).

0920-5861/$ – see front matter
doi:10.1016/j.cattod.2007.12.058

properties: $S_{BET} \sim 180\ m^2/g$ and pore volume $\sim 0.50\ cm^3/g$. However, few works have reported the use of ZrO_2/Al_2O_3 systems to support metallic particles. Dealing with Pd catalysts, there are not results in the opened literature. Souza et al. [21–23] prepared $Pt/ZrO_2/Al_2O_3$ catalysts with 1–20 wt.% ZrO_2 and observed that surface coverage of ZrO_2 on Al_2O_3 increased up to 10 wt.% of ZrO_2, falling above this concentration, due to the nucleation of ZrO_2 crystallites. The introduction of ZrO_2 in the Al_2O_3 surface occurs due to the formation of Zr–O–Al bonds, which strength decrease with the ZrO_2 content. The stronger Lewis acid sites decrease comparing to the weak ones when increasing the ZrO_2 content. The low acidic character of ZrO_2 increases the activity to dehydration and dehydrogenation reactions due to the reduction of cracking and coking side reactions [15,18,19].

Pd/ZrO_2 catalysts have been used in hydrogenation reactions, although few studies have been reported. Shen et al. [24] compared Pd catalysts in different supports in the CO hydrogenation. The activity and selectivity were distinct, depending on the supports characteristics. Higher CO conversions over Pd/ZrO_2 were ascribed to the presence of cationic Pd species formed through the metal–support interaction. In other study [16], the Pd/ZrO_2 system showed higher activity in the hydrogenation of phenol than other supports (MgO or Al_2O_3).

No references were found on the use of Pd/ZrO_2 catalysts for hydrogenation of styrene or PYGAS. The aim of this work was the development of Pd catalysts supported on ZrO_2/Al_2O_3, with different ZrO_2 loadings. These catalysts were tested in the hydrogenation of a mixture representative of PYGAS, containing styrene, 1,7-octadiene, 1-octene and dicyclopentadiene. The influence of reaction parameters (pressure and temperature) was evaluated.

2. Experimental

2.1. Preparation of supports and catalysts

Supports based on ZrO_2/Al_2O_3 were prepared in a rotatory evaporator by wet impregnation of an aqueous solution of zirconium acetate hydroxide ($Zr(C_2H_3O_2)_{1.4}(OH)_{2.6}$, Aldrich) and γ-Al_2O_3, considering 15 cm^3 of solution per gram of support, followed by calcination under dry air flow at 550 °C for 4 h. Supports presented 10 and 20 wt.% ZrO_2.

Zirconium oxide was prepared by addition of a 10% zirconium acetate hydroxide solution to a 5 M NH_4OH solution with pH control [25]. After digestion for 72 h at 90 °C, the precipitate was filtered, washed and calcined at 500 °C for 12 h (1 °C/min) with dry air flow.

Catalysts were prepared by dry impregnation with an aqueous solution of $PdCl_2$ (Acros) on γ-Al_2O_3 (Engelhard), ZrO_2, 10 wt.% ZrO_2/Al_2O_3 and 20 wt.% ZrO_2/Al_2O_3, yielding 1 wt.% Pd. After impregnation, the catalysts were dried at 120 °C for 16 h and calcined under dry air flow at 550 °C for 1 h.

2.2. Characterization

The elemental analysis of zirconium in the ZrO_2/Al_2O_3 supports and Pd in the catalysts was performed by X-ray fluorescence (XRF), using a Rigaku RIX 3100 equipment.

Specific surface areas (S) and pore volume (PV), calculated as 4 V/S_{BET}, were measured with a Micromeritcs Model ASAP 2000 equipment, using N_2 at −196 °C. Samples were outgassed for 18 h at 300 °C before the measurement of N_2 adsorption.

X-ray diffraction (XRD) measurements were carried out with the calcined samples and supports, using a Rigaku Miniflex diffractometer (voltage: 30 kV and current: 15 mA), equipped with a copper tube (λ = 1.5405 Å) and a graphite monochromator, operated in the step-scan mode 0.05° 2θ per step and counting for 2 s per step.

Diffuse reflectance spectroscopy (DRS) analyses were done on a Varian Cary 5 UV–vis–NIR spectrophotometer equipped with a Praying Mantis diffuse reflection device (Harrick^{TM}). Spectra were taken with the calcined catalysts, in the range of 200–800 nm. Supports were used as references.

Temperature programmed reduction (TPR) with H_2 used a quartz U-tube reactor with an on line thermal conductivity detector (TCD). Catalysts (0.5 g) were dried at 150 °C for 1 h under argon flow (AGA, 99.99%) and reduced with 1.6% H_2/Ar flow (30 cm^3/min) from 25 to 500 °C (10 °C/min). After reduction, samples were outgassed under argon flow at 500 °C for 30 min, cooled to 70 °C and then H_2 chemisorption measurements were performed. The amount of irreversible adsorbed H_2 was measured using the frontal method.

2.3. Hydrogenation of a model mixture

Hydrogenation tests were carried out in a batch reactor (Parr Instruments, Inc.) with a volume of 160 cm^3. Before each run, the catalyst (10 mg) was reduced with high purity hydrogen (AGA, 99.9999%) at 30 cm^3/min for 2 h under 130 °C (10 °C/min). After reduction, the reactor was cooled to the designed reaction temperature under H_2. A mixture (100 cm^3) of toluene (82.9% v/v), 1,7-octadiene (6.0% v/v), 1-octene (1.8% v/v), styrene (8.5% v/v) and dicyclopentadiene (DCPD, 0.8% v/v) was transferred to the reactor under inert atmosphere. This mixture was previously prepared and stored with molecular sieve in a refrigerator. Concentrations of mixture components were determined from typical pyrolysis gasoline composition [26]. The stirrer was set to 600 rpm and the pressure was increased by the introduction of H_2 in the reactor. Liquid samples were taken at regular intervals during 3 h and analyzed using a Hewlett-Packard gas chromatograph (HP6890 Plus) equipped with a column HP 1 (60 m) and FID detector.

3. Results and discussion

3.1. Catalysts' characterization

Table 1 shows the textural characterization of supports. Addition of ZrO_2 over Al_2O_3 caused an almost linear reduction on the surface area and pore volume of ZrO_2/Al_2O_3 in

Table 1
Textural characterization of supports

Support	S (m^2/g)	PV (cm^3/g)	D_P (Å)
Al_2O_3	220	0.50	97.3
$10ZrO_2/Al_2O_3$	177	0.42	95.2
$20ZrO_2/Al_2O_3$	156	0.38	97.0
ZrO_2	267	n.d.	n.d.

n.d.: not determined.

Table 2
Pd and ZrO_2 contents and DRS results

Catalyst	Pd (wt.%)	ZrO_2 (wt.%)	DRS attribution
Pd/Al_2O_3	1.0	0	PdO, $PdCl_2$, $Pd_xO_yCl_z$
$Pd/10ZrO_2/Al_2O_3$	1.1	9.5	PdO, $Pd_xO_yCl_z$
$Pd/20ZrO_2/Al_2O_3$	1.3	19.7	PdO, $PdCl_2$, $Pd_xO_yCl_z$
Pd/ZrO_2	1.0	99.0	PdO, $Pd_xO_yCl_z$

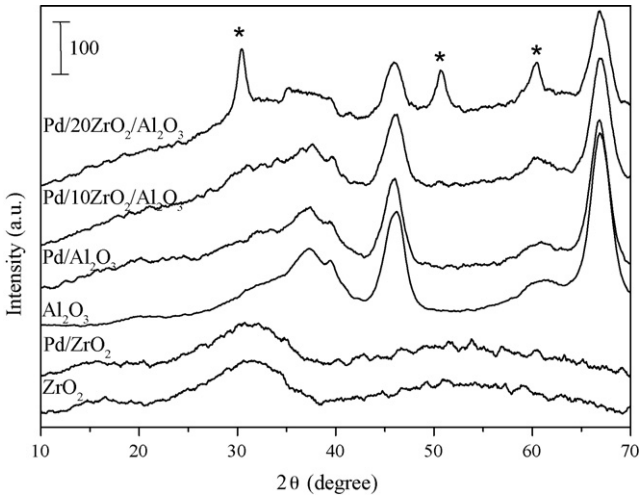

Fig. 2. XRD results of the Pd/$x$$ZrO_2/Al_2O_3$ catalysts and γ-Al_2O_3 support (*ZrO_2).

comparison with Al_2O_3. Results are similar to the literatures [18,22], ascribed to blockage of the Al_2O_3 pores by ZrO_2 crystallites. Other result observed in Table 1 was the pore volume reduction upon the addition of ZrO_2 to ZrO_2/Al_2O_3 support. However, the pore diameter was not changed significantly. The preparation method of ZrO_2 allowed obtaining a support with specific surface similar to Al_2O_3, according to the literature [25].

Pd and ZrO_2 contents, obtained by X-ray fluorescence (XRF) analysis, and diffuse reflectance spectroscopy (DRS) results of the calcined catalysts are presented in Table 2. DRS spectra are shown in Fig. 1. The wavelengths corresponding to the maximum intensity were obtained by gaussian decomposition of the spectra. The catalysts presented bands with maximum approximately at 280 and 420 nm. The first band is ascribed, according to Bozon-Verduraz et al. [27], to a superficial complex of Pd and chlorine, which can be reported as $Pd_xO_yCl_z$. The second band at 420 nm can be ascribed to bulk PdO particles without interaction with the support [17]. This band was more intense in the DRS spectrum of the Pd/ZrO_2 catalyst.

Pd/Al_2O_3 and $Pd/20ZrO_2/Al_2O_3$ catalysts also presented a band at 206 nm and a shoulder at 246 nm. The former was observed but not assigned by Rakai et al. [28] and it can be associated with the charge transfer (Pd → Cl) of $PdCl_2$. These authors also reported the shoulder at 246 nm after heating a $PdCl_2/Al_2O_3$ catalyst in oxygen, assigned to the charge transfer of Pd → O.

XRD diffractograms of Al_2O_3, ZrO_2 and calcined catalysts are presented in Fig. 2. Pd/Al_2O_3 and $Pd/10ZrO_2/Al_2O_3$ catalysts presented only crystalline γ-Al_2O_3 structure, with main peaks at $2\theta = 46^\circ$ (4 0 0) and 67° (4 4 0). The addition of 10 wt.% ZrO_2 caused no observable changes in the diffractogram of $Pd/10ZrO_2/Al_2O_3$ sample. Damyanova et al. [18] observed the formation of ZrO_2 crystallites with contents around 13–17 wt.% ZrO_2 in γ-Al_2O_3 (210 m^2/g). In fact, the 20 wt.% ZrO_2/Al_2O_3 presented intense peaks at $2\theta \approx 30.4^\circ$, 50.7° and 60.5°, ascribed to the tetragonal form of ZrO_2. The average crystallite size of ZrO_2 in $Pd/20ZrO_2/Al_2O_3$ catalyst was measured by Scherrer's equation with the peak at $2\theta \approx 30^\circ$, resulting 14 nm. This result is in agreement with the literature

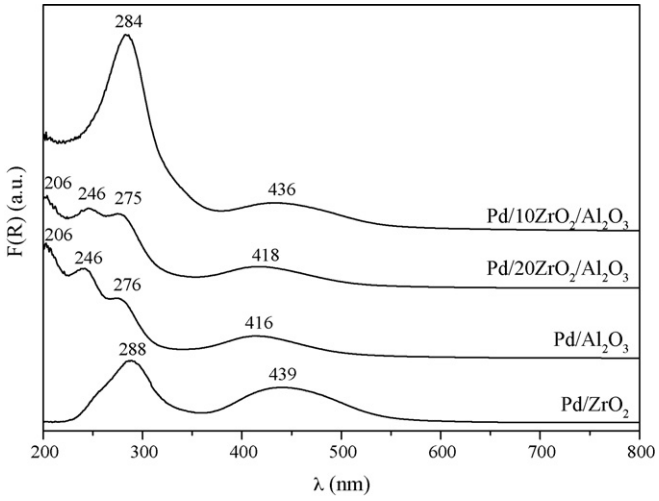

Fig. 1. DRS spectra.

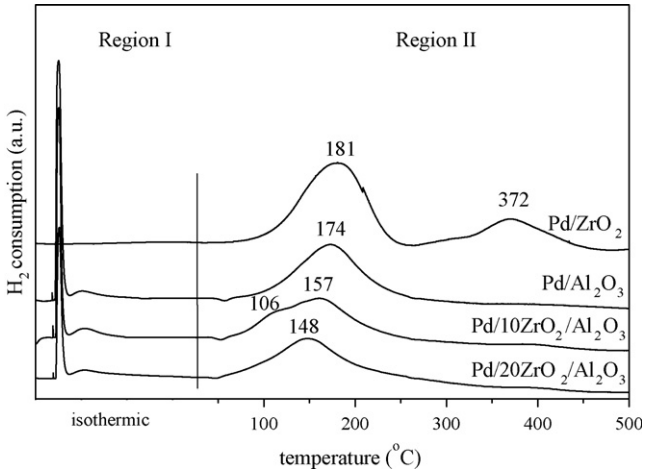

Fig. 3. TPR profiles of catalysts.

[29]. The Pd/ZrO_2 catalyst and the ZrO_2 support presented similar diffractograms, ascribed to amorphous ZrO_2.

Temperature programmed reduction (TPR) profiles with 1.74 vol.% H_2/Ar are shown in Fig. 3. The catalysts showed reduction peaks at room temperature and between 148 and 181 °C. A third peak was also observed, at 70 °C, ascribed to hydrogen desorption from the Pd β–H phase [30]. The increase of ZrO_2 content shifted the reduction temperature to lower values, suggesting modification of the Pd-support interaction. The $Pd/10ZrO_2/Al_2O_3$ catalyst presented a shoulder in the reduction profile at 106 °C, observed after gaussian deconvolution of the main peak at 157 °C. XRD analysis of the $Pd/10ZrO_2/Al_2O_3$ catalyst showed no crystalline ZrO_2 suggesting its dispersion on the Al_2O_3 surface. Thus, the shoulder in the reduction profile at 106 °C can be ascribed to Pd oxide supported in ZrO_2, whereas the peak at 157 °C can be attributed to PdO supported in Al_2O_3, as occurs in the other samples (Fig. 2). For the $20ZrO_2/Al_2O_3$, the presence of crystalline ZrO_2 was detected, characterizing high agglomeration degree. This result suggests that Pd oxide is mainly supported on Al_2O_3. Pd/ZrO_2 presented no reduction at room temperature. However, two peaks were verified, at 181 and 372 °C. Narui et al. [14] also observed absence of reduction of PdO supported on ZrO_2 at room temperature, attributing this result to the stability of Pd oxide on this support.

Quantitative results of TPR were divided in two regions: at room temperature (I) and during heating the sample (II). Table 3 shows the percentage of reduction during heating (region II). Pd/Al_2O_3 and $Pd/20ZrO_2/Al_2O_3$ catalysts showed similar H_2 consumption in this region (94–95%), whereas $Pd/10ZrO_2/Al_2O_3$ catalyst presented lower reduction under this condition. This result suggests smaller Pd particles in the first two samples, probably resulting higher metallic dispersion. For the Pd/ZrO_2 catalyst, the complete reduction of Pd oxide occurs at 181 °C. Thus, the second peak, at 372 °C, can be tentatively ascribed to the reduction of ZrO_2.

H_2 chemisorption experiments were carried out in order to determine the metallic dispersion of the catalysts. The results, expressed as metallic dispersion, are shown in Table 3. The Pd/Al_2O_3 catalyst presented higher dispersion than the $Pd/10ZrO_2/Al_2O_3$ sample. High Pd dispersion has been associated with the literature to the presence of oxychoroPd surface complex supported on Al_2O_3, like $Pd_xO_yCl_z$, present in both catalysts [17,32,33]. Pd smaller dispersion over ZrO_2 must be associated with low stability of oxychoroPd surface complex during heating in TPR analysis, due to Al_2O_3 surface covering by ZrO_2. In fact, Souza et al. [22] suggested that ZrO_2 retains less chlorine in its surface than Al_2O_3.

Table 3
H_2 consumption and dispersion of the catalysts

Catalyst	H_2(I)[a]	H_2(II)[a]	Reduction (%)	D_{H_2} (%)
Pd/Al_2O_3	0.46	8.43	95	62.2
$Pd/10ZrO_2/Al_2O_3$	1.14	8.31	100	52.5
$Pd/20ZrO_2/Al_2O_3$	0.51	8.73	98	n.d.
Pd/ZrO_2	0	9.91	100	39.0

n.d.: not determined.
[a] H_2 consumption ($\mu molH_2/mgPd$).

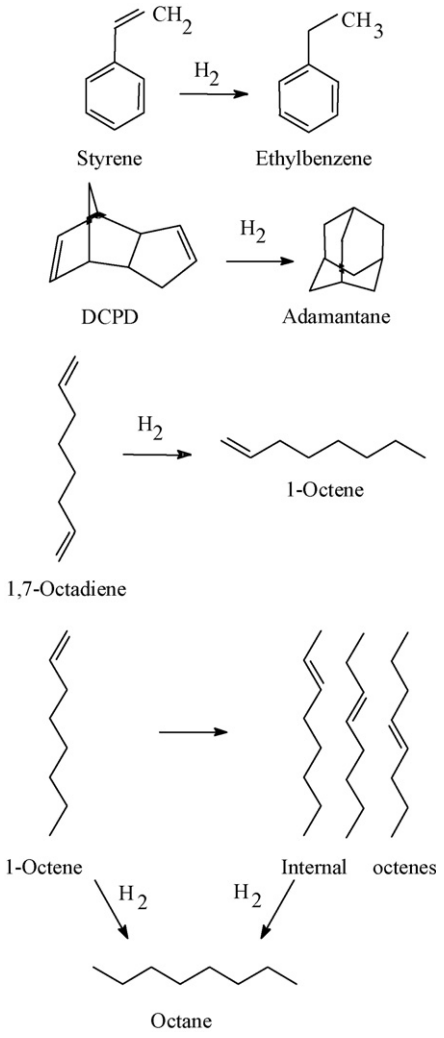

Fig. 4. Reaction scheme for the hydrogenation of a model mixture.

3.2. Hydrogenation of the model mixture

Results of the model mixture hydrogenation were expressed as molar fraction of components (toluene, 1,7-octadiene, 1-octene, styrene and DCPD). Fig. 4 represents the reaction pathways of styrene to ethyl-benzene, DCPD to adamantine, 1,7-octadiene to 1-octene and 1-octene to octane.

In the hydrogenation of pyrolysis gasoline, the main reactions of interest are conversion of styrene to ethyl-benzene and the removal of di-olefin. The hydrogenation of aromatic rings for the formation of cyclo-hexanes must be minimized [31]. In our studies we did not observe the formation of cyclo-hexanes in appreciable amount, while the formation of internal octenes was significant. Figs. 5–7 show the behavior of styrene and DCPD conversion and the octane molar fraction during the reaction. Initial reaction rates shown in Fig. 8, were obtained via derivative of fitted conversion versus time curve, carried out at 30 bar and 60 °C. Octane molar fraction was used to represent the conversion of 1,7-octadiene and 1-octene to the corresponding paraffin.

The hydrogenation rate of styrene was the greater one. For example, the Pd/Al_2O_3 catalyst presented reaction rates of 213,

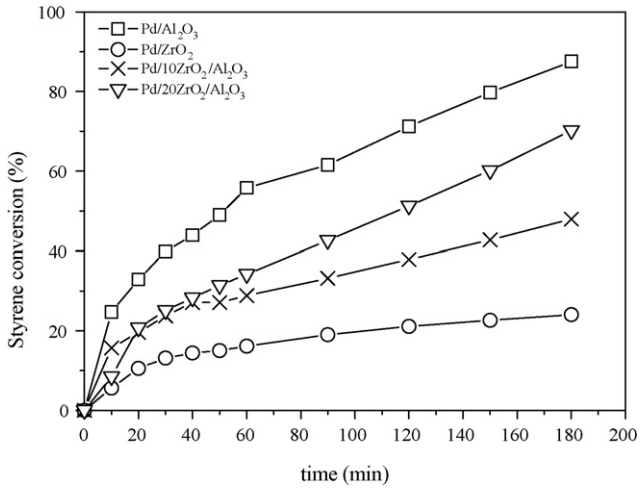

Fig. 5. Styrene conversion vs. reaction time.

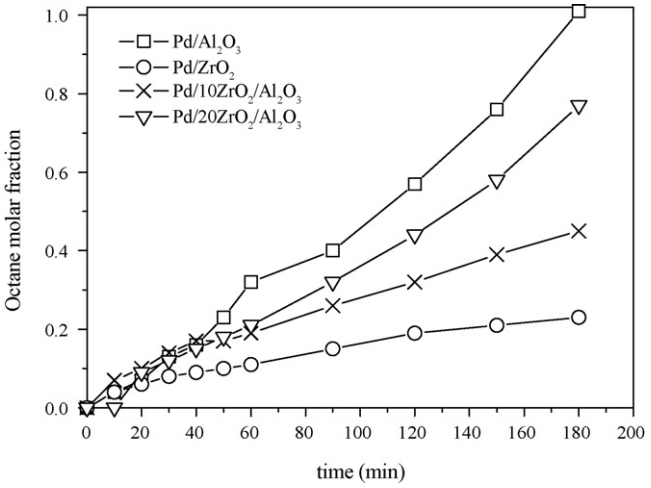

Fig. 7. Octane molar fraction vs. reaction time.

15 and 1.9 mol/(kg_{cat} min) for the hydrogenation of styrene and DCPD and the octane formation, respectively. According to Hoffer et al. [31], the greater rate for the styrene hydrogenation must be related to the highest adsorption strength of this compound in comparison, for example, to 1-octene in a Langmuir–Hinshelwood kinetic model.

As shown in Fig. 8, the initial reaction rates of styrene and DCPD for the tested catalyst decreased in the same order. Pd/Al_2O_3 showed the highest activity. The increase of ZrO_2 content reduced the catalysts' activity. This reduction in the activity followed the decrease in the dispersion of Pd particles, obtained by H_2, chemisorption, Table 3.

Well-dispersed Pd particles have been associated in literature to the presence of superficial complexes in Al_2O_3, represented as $Pd_xO_yCl_z$ [17,32,33]. This species was observed by DRS in all catalysts. Thus, the lower dispersion observed for catalysts prepared with ZrO_2 and ZrO_2/Al_2O_3 is associated with the low stability of these superficial complexes in ZrO_2 as compared to Al_2O_3.

In agreement to reaction schemes proposed in the literature [31], the hydrogenation of di-olefins can result the corresponding mono-olefin and isomers, as represented in Fig. 4. In order to examine the hydrogenation pathway of di-olefin under prevailing conditions, experiments with a mixture containing only toluene and 1,7-octadiene were carried out for the same conditions used with the mixture model, using the Pd/Al_2O_3 and Pd/ZrO_2 catalysts. Molar percentages of 1,7-octadiene,

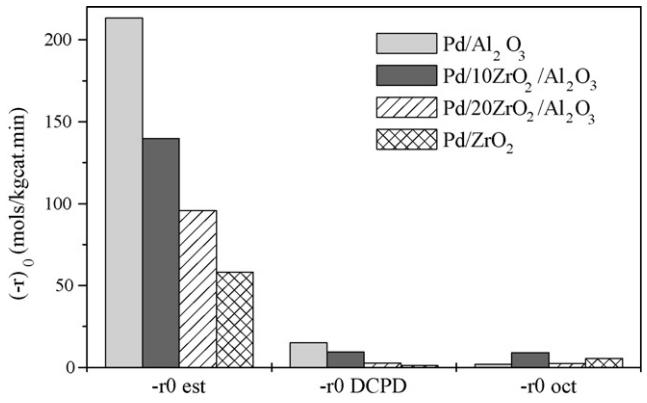

Fig. 8. Initial reaction rates ($T = 60$ °C, $P = 30$ bar and $m_{cat} = 10$ mg).

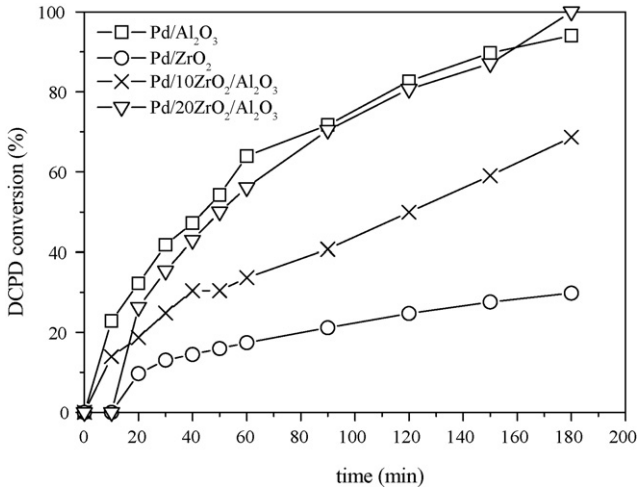

Fig. 6. DCPD conversion vs. reaction time.

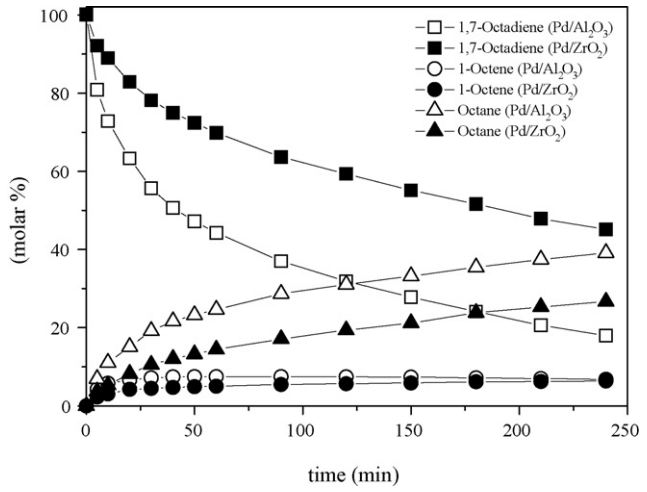

Fig. 9. 1,7-Octadiene, 1-octene and octane molar percentages vs. reaction time.

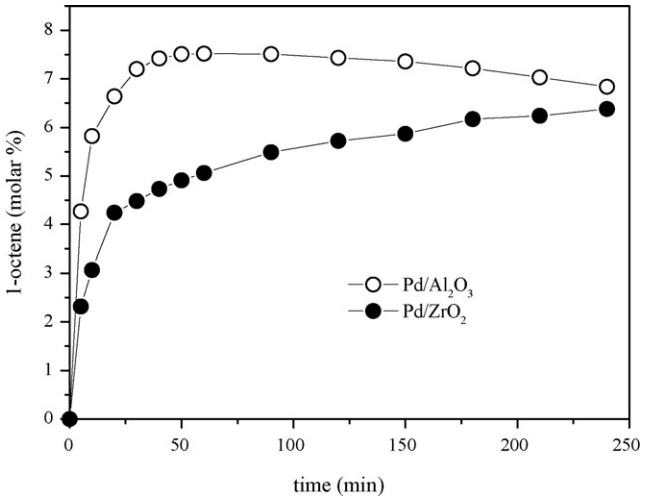

Fig. 10. 1-Octene molar percentage vs. reaction time.

1-octene and octane during experiment are shown in Fig. 9. It was observed that the conversion of 1,7-octadiene yields predominantly octane. However, it was also verified the formation of 1-octene and internal octenes. This result suggests that 1-octene is formed in the hydrogenation of 1,7-octadiene. Subsequently, octane is formed through a mechanism in series, nevertheless it is also possible the direct reaction of 1,7-octadiene to octane. Di Serio et al. [34] verified that in the hydrogenation of molecules such as 1,7-octadiene, the isomerization to iso-octadiene, the formation of mono-olefins and finally octane occur.

Fig. 10 detaches the 1-octene low concentration region. The molar percentage of 1-octene, originated from the hydrogenation of 1,7-octadiene, for the Pd/Al_2O_3 catalyst, increased up to 50 min and then decreased, characterizing its consumption for octane formation, as a result, the sequence of reactions in series. Dobrovolná et al. [35] studied competitive hydrogenation of alkenes, dienes and alkynes using Pd catalysts. The authors reported that 1,7-octadiene hydrogenation coursed through 1-octene that is partially isomerized to *cis* and *trans*-2-octene and later, hydrogenated to octane.

4. Conclusions

Pd catalysts supported on Al_2O_3, ZrO_2 and ZrO_2/Al_2O_3 presented distinct behavior regarding reducibility with H_2 and Pd dispersion. For the Pd/ZrO_2, Pd interacted strongly with the support, with a poor dispersion as compared to Pd/Al_2O_3. For the $Pd/10ZrO_2/Al_2O_3$ catalyst, Pd interacted with ZrO_2 and Al_2O_3. Hydrogenation of a mixture of styrene, dicyclopentadiene (DCPD), 1,7-octadiene and 1-octene in a batch reactor showed that the initial rate of hydrogenation of styrene was the higher one. Hydrogenation of 1,7-octadiene to octane occurs via series reaction, with 1-octene as intermediate. The most active catalyst was the Pd/Al_2O_3, which presented the highest dispersion.

Acknowledgements

The authors acknowledge Fundação de Amparo à Pesquisa (FAPERJ) for financial support. Gabriel Rosa dos Santos thanks Conselho Nacional de Desenvolvimento Científico e Tecnológico (CNPq) for the scholarship received during this work. The authors acknowledge Núcleo de Catálise/PEQ/COPPE/UFRJ (Brazil) for the characterization analyses.

References

[1] A.B. Gaspar, M.A.P. Silva, O.Q.F. Araújo, J.L. Medeiros, J.M. Britto, in: Proceedings of the AIChE 2003 Spring Nat. Meeting, New Orleans, (2003), p. 630.
[2] Y.M. Cheng, J.R. Chang, J.C. Wu, Appl. Catal. A 24 (1986) 273.
[3] Shell Development Co., Hydrocarbon Proc. (9) (1982) 126.
[4] M.C. Sze, W.V. Bauer, Chem. Eng. Prog. 2 (1969) 59.
[5] P. Castaño, B. Pawelec, J.L.G. Fierro, J.M. Arandes, J. Bilbao, Appl. Catal. A: Gen. 315 (2006) 101.
[6] C. Ringelhan, G. Burgfels, J.G. Neumayr, W. Seuffert, J. Klose, V. Kurth, Catal. Today 97 (2004) 277.
[7] T.A. Nijhuis, F.M. Dautzenberg, J.A. Moulijn, Chem. Eng. Sci. 58 (2003) 1113.
[8] V.I. Pârvulescu, G. Filoti, V. Pârvulescu, N. Grecu, E. Angelescu, I.V. Nicolescu, J. Mol. Catal. A 89 (1994) 267.
[9] V.L. Barrio, P.L. Arias, J.F. Cambra, M.B. Güemez, B. Pawelec, J.L.G. Fierro, Appl. Catal. A 242 (2002) 17.
[10] B.W. Hoffer, F. Devred, P.J. Kooyman, A.D. Van Langeveld, R.L.C. Bonn, C. Griffiths, C.M. Lok, J.A. Moulijn, J. Catal. 209 (2002) 245.
[11] P. Kačer, L. Červený, J. Mol. Catal. A 212 (2004) 183.
[12] S.D. Jackson, L.A. Shaw, Appl. Catal. A 134 (1996) 91.
[13] R.V. Chaudhari, R. Jaganathan, D.S. Kolhe, G. Emig, F. Hofmann, Chem. Eng. Sci. 41 (1986) 3073.
[14] K. Narui, K. Furuta, H. Yata, A. Nishida, Y. Kohtoku, T. Matsuzaki, Catal. Today 45 (1998) 173.
[15] S. De Rossi, G. Ferraris, S. Fremiotti, V. Indovina, A. Cimino, Appl. Catal. A 106 (1993) 125.
[16] S. Velu, M.P. Kapoor, S. Inagaki, K. Suzuki, Appl. Catal. A 245 (2003) 317.
[17] A.B. Gaspar, L.C. Dieguez, J. Catal. 220 (2003) 309.
[18] S. Damyanova, P. Grange, B. Delmon, J. Catal. 168 (1997) 421.
[19] J.M. Dominguez, J.L. Hernandez, G. Sandoval, Appl. Catal. A 197 (2000) 119.
[20] T. Klimova, M.L. Rojas, P. Castillo, R. Cuevas, J. Ramírez, Microporous Mesopororous Mater. 20 (1998) 293.
[21] D.A.G. Aranda, M. Schmal, M.M.V.M. Souza, C. Perez, Stud. Surf. Sci. Catal. 132 (2001) 695.
[22] M.M.V.M. Souza, D.A.G. Aranda, C. Perez, M. Schmal, Phys. Stat. Sol. A: Appl. Res. 187 (2001) 297.
[23] M.M.V.M. Souza, D.A.G. Aranda, M. Schmal, J. Catal. 204 (2001) 498.
[24] W.J. Shen, M. Okumura, Y. Matsumura, M. Haruta, Appl. Catal. A 213 (2001) 225.
[25] G.K. Chuah, S. Jaenicke, K.S. Chan, Appl. Catal. A: Gen. 145 (1996) 267.
[26] J. Cosyns, L. Quicke, Q. Debuisschert. Pygas Upgrading, IFP North America, Inc., www.ifpna.com, 2001.
[27] F. Bozon-Verduraz, A. Omar, J. Escard, B. Pontvianne, J. Catal. 53 (1978) 126.
[28] A. Rakai, D. Tessier, F. Bozon-Verduraz, New J. Chem. 16 (1992) 869.
[29] P. Rao, M. Iwasa, J. Wu, J. Ye, Y. Wang, Ceram. Int. 30 (2004) 923.
[30] W.-J. Shen, M. Okumura, Y. Matsumura, M. Haruta, Appl. Catal. A 213 (2001) 225.
[31] B.W. Hoffer, R.L.C. Bonne, A.D. van Langeveld, C. Griffiths, C.M. Lok, J.A. Moulijn, Fuel 83 (2004) 1.
[32] Y. Shen, L. Cai, J. Li, S. Wang, K.H. Huang, Catal. Today 6 (1989) 47.
[33] D.O. Simone, T. Kennelly, N.L. Brungard, R.J. Farrauto, Appl. Catal. A: Gen. 70 (1991) 87.
[34] M. Di Serio, V. Balato, A. Dimiccoli, L. Maffucci, P. Iengo, E. Santacesaria, Catal. Today 66 (2001) 403.
[35] Z. Dobrovolná, P. Kacer, L. Cervený, J. Mol. Catal. 130 (1998) 279.